

# A Comprehensive Differential Proteomic Study of Nitrate Deprivation in *Arabidopsis* Reveals Complex Regulatory Networks of Plant Nitrogen Responses

Xu Wang,<sup>†,‡,§</sup> Yangyang Bian,<sup>||</sup> Kai Cheng,<sup>||</sup> Hanfa Zou,<sup>\*,||</sup> Samuel Sai-Ming Sun,<sup>\*,§</sup> and Jun-Xian He<sup>\*,§</sup>

<sup>†</sup>School of Life Sciences, Tsinghua University, Beijing 100084, China

<sup>‡</sup>Division of Life Sciences, Graduate School at Shenzhen, Tsinghua University, Shenzhen, Guangdong 518055, China

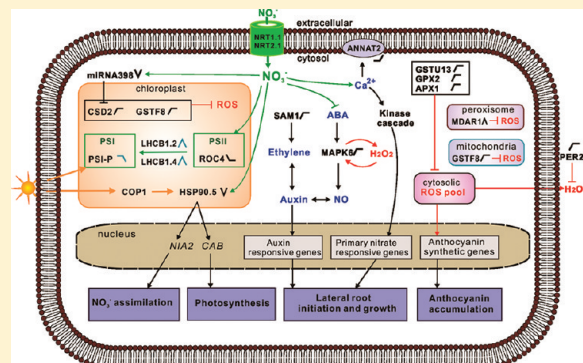
<sup>§</sup>State Key Laboratory of Agrobiotechnology and School of Life Sciences, The Chinese University of Hong Kong, Shatin, N.T., Hong Kong SAR, China

<sup>||</sup>Key Laboratory of Separation Sciences for Analytical Chemistry, National Chromatographic R&A Center, Dalian Institute of Chemical Physics, Chinese Academy of Sciences, Dalian 116023, China

## Supporting Information

**ABSTRACT:** Nitrogen (N) is an important nutrient and signal for plant growth and development. However, to date, our knowledge of how plants sense and transduce the N signals is very limited. To better understand the molecular mechanisms of plant N responses, we took two-dimensional gel-based proteomic and phosphoproteomic approaches to profile the proteins with abundance and phosphorylation state changes during nitrate deprivation and recovery in the model plant *Arabidopsis thaliana*. After 7-day-old seedlings were N-deprived for up to 48 h followed by 24 h recovery, a total of 170 and 38 proteins were identified with significant changes in abundance and phosphorylation state, respectively. Bioinformatic analyses implicate these proteins in diverse cellular processes including N and protein metabolism, photosynthesis, cytoskeleton, redox homeostasis, and signal transduction. Functional studies of the selected nitrate-responsive proteins indicate that the proteasome regulatory subunit RPT5a and the cytoskeleton protein Tubulin alpha-6 (TUA6) play important roles in plant nitrate responses by regulating plant N use efficiency (NUE) and low nitrate-induced anthocyanin biosynthesis, respectively. In conclusion, our study provides novel insights into plant responses to nitrate at the proteome level, which are expected to be highly useful for dissecting the N response pathways in higher plants and for improving plant NUE.

**KEYWORDS:** proteomics, phosphoproteomics, nitrogen (N), nitrate, N signaling, N use efficiency, *Arabidopsis thaliana*



## INTRODUCTION

Nitrogen (N) is an essential macronutrient required for plant growth and development and a key limiting factor for agriculture productivity.<sup>1–3</sup> Among the available N forms (nitrate, ammonium, amino acid, peptides, etc.), nitrate is the most abundant N source for plants.<sup>1,4</sup> Since nitrate in soil is readily dissolved in water and lost,<sup>4</sup> plants are frequently subjected to N limiting conditions and millions of tons of N fertilizers have to be applied to the field every year worldwide to ensure agriculture productivity. However, due to the current low nitrogen use efficiency (NUE) of crop plants (30–50%),<sup>5</sup> most of the N fertilizers supplied are lost by leaching into the soil, water, and air and have imposed deleterious environmental effects.<sup>6</sup> Therefore, increasing the NUE of crop plants and reducing N fertilizer usage are highly desirable for both a productive and sustainable agriculture.

Not only is nitrate a major nutrient for plants, it also serves as a signaling molecule.<sup>7,8</sup> For instance, nitrate affects root morphology by suppressing root growth at high concentrations and enhancing at low concentrations independent of nitrate assimilation.<sup>9</sup> Primary nitrate response is the best known nitrate-induced response, in which genes encoding the nitrate assimilatory enzymes and nitrate transporters are rapidly induced by nitrate. Besides, transcriptomic studies<sup>10–12</sup> have indicated that many other genes for diverse biological processes such as amino acid and nucleic acid metabolisms, protein folding, RNA processing, and hormone biosynthesis could also be rapidly induced or repressed by nitrate. However, since mRNA abundance may only represent putative function of genes, whether these

Received: October 28, 2011

Published: February 14, 2012

nitrate effects at the transcriptional level reflect its effect at protein level and lead to different N responses is a question of concern.

In bacteria, nitrate is signaled through a His-to-Asp phosphorelay system, and the environmental nitrate is sensed by a pair of transmembrane histidine kinases.<sup>13</sup> The N signaling system is also well characterized in fungi as well as in unicellular alga. Fungi sense environmental ammonium by high-affinity ammonium transporters and N signaling specific GATA transcription factors are involved.<sup>14</sup> In the algae *Chlamydomonas*, nitrate signaling requires the regulatory gene *NIT2*.<sup>15</sup> The most significant advance in our understanding of nitrate signaling mechanisms in higher plants has been the discovery of the *Arabidopsis* nitrate dual-affinity transporter NRT1.1/CHL1 as a nitrate sensor.<sup>16,17</sup> By using an uptake- and sensing-decoupled *chl* mutant in *Arabidopsis*, Ho et al. demonstrated that CHL1 employs dual-affinity binding and a phosphorylation switch to sense a wide range of nitrate concentrations in the soil.<sup>16</sup> There was evidence showing that the *Arabidopsis* nitrate transporter NRT2.1 could also act as a nitrate sensor.<sup>18,19</sup> Other N signaling players in plants were identified by transcriptome and comparative genomic approaches, which include the NIN-like protein 7 (NLP7), a homologue of the fungus nitrate assimilation regulatory protein NIN in *Arabidopsis*,<sup>20</sup> CIPK8,<sup>21</sup> ANR1,<sup>22</sup> CCA1,<sup>23</sup> and microRNAs (miR393 and miR167,<sup>24</sup> miR169 and miR398<sup>25</sup>). By using a forward genetic approach, a RING-type ubiquitin E3 ligase NLA (nitrogen limitation adaptation) was identified as a positive regulator of *Arabidopsis* adapting to low-nitrate conditions.<sup>26,27</sup>

In addition to transcriptomic studies, proteomics approaches have also been applied in bacteria,<sup>28</sup> fungi,<sup>29,30</sup> and plants<sup>31–33</sup> to detect their responses to different N conditions at protein level. For example, the response of whole plant proteome to different nitrate levels have been studied in *Zea mays*,<sup>31</sup> *Hordeum vulgare*,<sup>32</sup> and *Triticum aestivum*.<sup>33</sup> However, due to the small number of proteins identified from these studies, the regulatory mechanisms of plant N responses at the protein level remain poorly understood. In addition, since the N-related transcriptomic and metabolomic studies<sup>10–12,34</sup> have been done most extensively in *Arabidopsis* and the known molecular mechanisms of plant N responses were primarily achieved by studies in *Arabidopsis* as well, it is essential to carry out parallel proteomic analyses in *Arabidopsis* to gain a multilevel understanding of plant N responses.

Here, the two-dimensional gel electrophoresis (2DE)-coupled MS/MS analysis was employed to comprehensively evaluate the proteomic response of *Arabidopsis* plants to nitrate deprivation and recovery. By using three different staining methods, we identified 170 nitrate responsive proteins with abundance changes and 38 proteins with phosphorylation changes. Bioinformatics and gene functional studies revealed a close linkage between the protein changes and the overall plant nitrate responses. These results provided novel insights into the molecular mechanisms of plant N responses and expanded our toolbox for genetic manipulation of plant NUE.

## MATERIALS AND METHODS

### Plant Materials and Growth Conditions

All the 2-DE experiments in this study were performed on the *Arabidopsis thaliana* ecotype Columbia (Col-0). Most of the transgenic plants used were also in the Col-0 background, except the two mutant alleles of the 26S proteasome AAA-ATPase Regulatory Particle 5a (RPT5a), *rpt5a-2* and *rpt5a-3*, which were in the Wassilewskija (Ws) background.<sup>35</sup>

For 2-DE experiments, plants were grown hydroponically as described before<sup>12</sup> with minor modifications. Briefly, sterilized Col-0 *Arabidopsis* seeds were imbibed in sterile full N (+N) media [half-strength MS medium without N (Caissonlabs), 3 mM MES, 0.5% sucrose, 5 mM KNO<sub>3</sub>, pH 5.7] at a ratio of 10 mg of seeds/100 mL of media. Seeds were cold-treated at 4 °C for 2 days to synchronize germination and germinated seeds were grown under continuous light of 50 μmol s<sup>-1</sup> m<sup>-2</sup> around flasks and temperature at 22 °C in an Innova 4340 illuminated shaker (New Brunswick Scientific) at a speed of 90 rpm. After 7 d, the media were changed in all flasks; some received 100 mL of 1/2 MS (+N) media as the control while others received N free (−N) media (no KNO<sub>3</sub>, which was replaced by 5 mM KCl) for N deprivation. On day 8 (24 h after N deprivation), the media were renewed in all flasks. On day 9 (48 h after N deprivation), the media in some of the −N flasks were changed into +N media for recovery and the media in other flasks were renewed with N-free media. Seedlings were harvested at 0, 3, 6, 12, 24, 48, 72 h of N deprivation, and 3, 6, 12, 24 h after nitrate refeeding. The corresponding +N controls were harvested at the same time points. Harvested materials were immediately frozen in liquid N<sub>2</sub> and stored at −80 °C for subsequent use.

### Physiological Measurements

Fresh weight of seedlings was measured by using an analytical balance and primary root length was determined by image analysis using the ImageJ software version 1.41 (<http://rsb.info.nih.gov/ij/>). Total protein was prepared by trichloroacetic acid (TCA)/acetone precipitation method<sup>36</sup> and the protein concentration was determined by the modified Bradford method<sup>37</sup> using bovine serum albumin (BSA; Bio-Rad) as standard. The procedure of Fitter et al.<sup>38</sup> was followed for extraction and quantification of shoot chlorophylls and anthocyanin levels in shoot were measured according to Sunkar et al.<sup>39</sup> Nitrate content in plants was measured by high-performance liquid chromatography (HPLC) using an Agilent ZORBAX SB-C18 HPLC column (5 μm, 80 Å, 250 × 4.6 mm i.d.) in an Agilent 1100 HPLC system (Supplemental Experimental Procedures in Supporting Information).

### Total Protein Extraction and two-Dimensional Gel Electrophoresis

Total protein was extracted by the phenol–methanol method<sup>40</sup> with modified SDS Extraction Buffer [100 mM Tris-HCl, pH 8.0, 2% (w/v) sodium dodecyl sulfate (SDS), 1% β-mercaptoethanol, 5 mM EGTA, 10 mM EDTA, 0.4% protease inhibitor cocktail for plant materials (Sigma), 25 mM sodium fluoride, and 1 mM sodium orthovanadate]. The final protein pellet was resuspended in Sample Buffer (7 M urea, 2 M thiourea, 4% CHAPS, and 20 mM dithiothreitol (DTT)). The protein concentration was quantified with Bradford method<sup>37</sup> using BSA as standard. Total protein at 125 or 800 μg was used for silver or ProQ/CBB staining and the sample volume was brought to 350 μL by adding Sample Buffer, in which the IPG buffer, pH 4–7 (GE Healthcare), was added to a final concentration of 0.5%. The samples were then applied to Immobiline DryStrips pH 4–7, 18 cm (GE Healthcare). Isoelectric focusing (IEF) was carried out on an Ettan IPGphor 3 (GE Healthcare) at 20 °C using a maximal current of 50 μA/strip and the settings below. For the 125 μg protein loading, samples were rehydrated for 2 h and IEF was run at 40 V for 10 h, 300 V for 3 h, 1000 V for 1 h, with gradient increase to 8000 V in 3 h, and remained at 8000 V until reaching 40 000 Vh (total ~56 000 Vh). For the 800 μg protein loading, rehydration for 2 h and then IEF at 40 V for 10 h, 300 V for 5 h, 1000 V for 1 h,

with gradient increase to 8000 V in 3 h, and remained at 8000 V until reaching 70 000 Vh (total ~86 000 Vh). After IEF, IPG strips were sequentially equilibrated in Equilibration Buffer [6 M urea, 30% glycerol, 2% (w/v) SDS, 50 mM Tris-HCl, pH 8] supplemented with 1% DTT or 2.5% iodoacetamide, each for 15 min. The strips were then transferred to 12.5% SDS-PAGE gels for second-dimension electrophoresis using the Ettan DALTsix Large Vertical System (GE Healthcare). SDS-PAGE was run at 1 W/gel for 2 h and then 3 W/gel for 12–16 h until the bromophenol blue dye front reached the lower end of the gel.

### Gel Staining, Image Scanning, and Analysis

The silver staining procedure compatible with MS analysis was carried out as described previously.<sup>41</sup> Six biological replicates were applied to each treatment and each biological replicate contained two technical replicates in 2-DE (a total of 120 silver-stained 2-DE gels). Phosphoprotein staining was performed using the Pro-Q diamond phosphoprotein stain (Invitrogen) as described elsewhere,<sup>42</sup> and the same gels were then stained with colloidal CBB (G250)<sup>43</sup> for spot picking and MS identification of the ProQ-stained protein spots. CBB staining was also used to quantify protein abundance changes between treatments and controls. Three biological replicates were applied to each treatment and each biological replicate contained two technical replicates in 2-DE (a total of 18 ProQ/CBB-stained 2-DE gels). The silver- and CBB-stained gels were scanned using an ImageScanner (GE Healthcare) at a 300 dpi resolution. The ProQ-stained gels were imaged with a Typhoon Trio Imager (GE Healthcare) with 532 nm excitation source and 555 nm emission filter at 100  $\mu$ m resolution and the phosphorylation level was determined by the spot intensity on gel images. Gel images from silver, CBB, and ProQ-staining were all analyzed using the ImageMaster 2D Platinum software version 5.0 as described in the user manual (GE Healthcare). Background subtraction and normalization were done fully automatically. Minimal manual editing was performed to ensure that spots were correctly matched between gels. For silver-stained gels, the N deprivation versus +N control at 6, 24, 48, 72 h, and nitrate refeeding versus 48 h N deprivation at 6, 24 h (R6h, R24h) were analyzed for their 2-DE patterns and their protein spots by relative spot volume (%Vol). Using paired Student's *t*-test, only spots showing significant changes (%Vol varied more than 1.5-fold,  $p < 0.5$ ) were selected for further identification. For ProQ and CBB-stained gels, only N deprivation versus +N control at 48 h, and nitrate readdition at 24 h (R24h) versus N deprivation at 48 h were analyzed and spots showing significant changes (%Vol varied more than 1.5-fold,  $p < 0.5$  by paired Student's *t*-test) were selected for further identification.

### In-Gel Tryptic Digestion, Mass Spectrometry, and Database Searching

Silver and CBB-stained protein spots of interest were excised manually and subjected to in-gel digestion. The images of ProQ-stained gels were manually compared with the images of the same gels stained with CBB and ProQ-stained spots of interest were excised from the corresponding CBB gels. For silver-stained spots, gel pieces were digested as described previously.<sup>41</sup> For CBB-stained spots, gel pieces were first destained in 25 mM ammonium bicarbonate and 50% methanol several times until gel pieces turned colorless. Gel pieces were then rinsed and dehydrated by 100% acetonitrile (ACN). Following vacuum-drying, gel pieces were digested with 20  $\mu$ g/mL sequencing grade trypsin (Promega) in 25 mM ammonium bicarbonate, pH 8.0, for 16 h at 37 °C.

Tryptic peptides were extracted with 2.5% trifluoroacetic acid (TFA) and 50% ACN.

Mass spectrometric analysis was carried out using a MALDI-TOF/TOF tandem mass spectrometer ABI 4700 proteomics analyzer (Applied Biosystems, Foster City, CA). Briefly, mass data acquisitions were piloted by 4000 Series Explorer Software v3.0 using batched-processing and automatic switching between MS and MS/MS modes. The MS and MS/MS data were loaded into the GPS Explorer software v3.5 (Applied Biosystems, Foster City, CA) and searched against the NCBI database (released on March 5, 2010; including 10 544 437 sequences, 3 594 124 216 residues) with species restriction to *A. thaliana* (42 994 sequences) by Mascot search engine version 2.1 (Matrix Science, London, U.K.). Details of the procedures used are given in Supplemental Experimental Procedures (Supporting Information).

### Phosphorylation Site Mapping

The total proteins prepared for 2DE from the 48 h N-deprived, 48 h N-replete, and 24 h recovered seedlings were respectively diluted in Reducing Buffer containing 100 mM NH<sub>4</sub>HCO<sub>3</sub> (pH 8.2) and 8 M urea and the concentration was determined by Bradford assay<sup>37</sup> using BSA as a standard. The mixture (500  $\mu$ g of proteins) was reduced using 10 mM DTT at 60 °C for 1 h and then alkylated using 20 mM iodoacetamide (IAA) in the darkness at room temperature for 30 min. After that, 100 mM NH<sub>4</sub>HCO<sub>3</sub> buffer (pH 8.2) was added until the protein concentration was about 1 mg/mL. Then, trypsin was added with an enzyme-to-protein ratio of 1/25 (w/w) and the digestion was performed at 37 °C overnight. The phosphopeptides were enriched by Ti<sup>4+</sup>-IMAC microspheres.<sup>44</sup> For the mass spectrometric analysis, the enriched phosphopeptides or reconstituted tryptic peptides from 2DE gel spots were redissolved in 0.1% FA solution and analyzed in a LTQ linear IT mass spectrometer (Thermo, CA).<sup>45</sup> For the database search, the peak lists for MS<sup>2</sup> and MS<sup>3</sup> were generated by Bioworks (Thermo, version 3.3.1 SP1) and the spectra were searched using SEQUEST against a nonredundant *Arabidopsis* protein database (TAIR10, Nov 2010 released, including 27 416 entries) including both original database and the reversed complement. The software named Armone was applied to filter the identifications to achieve false discovery rate (FDR) <1% at peptide level.<sup>46,47</sup> Details of the procedures used are given in Supplemental Experimental Procedures (Supporting Information).

### Bioinformatic Analysis

The protein functions were assigned using the *Arabidopsis* genome annotation database (TAIR10), Gene Ontology Annotation (GOA) Database, and InterPro database version 31.0. In the case of the same protein being identified in multiple spots with differential accumulation, the proteins were listed as independent entities. The CAST (Clustering Affinity Search Technique) was used to summarize the abundance changes of all identified proteins by using the MeV (Multi Experiment Viewer) software version 4.6.<sup>48</sup> The quantitative protein data of each treatment were taken as fold changes of abundance in comparison to its corresponding "control" (for N deprivation samples, the plant grown under +N condition at each time-point was the control, and for nitrate refeeding samples, samples at the 48 h of N deprivation was the control). Then, the data were log2-transformed and zero was assigned for fold changes less than 1.5 or not significant ( $p \geq 0.05$ ) (Supplemental Table 4). During the analysis, the Pearson correlation and threshold parameter of 0.8 were applied. Cytoscape version 2.6.3 along with its plugin Bingo version 2.3 were

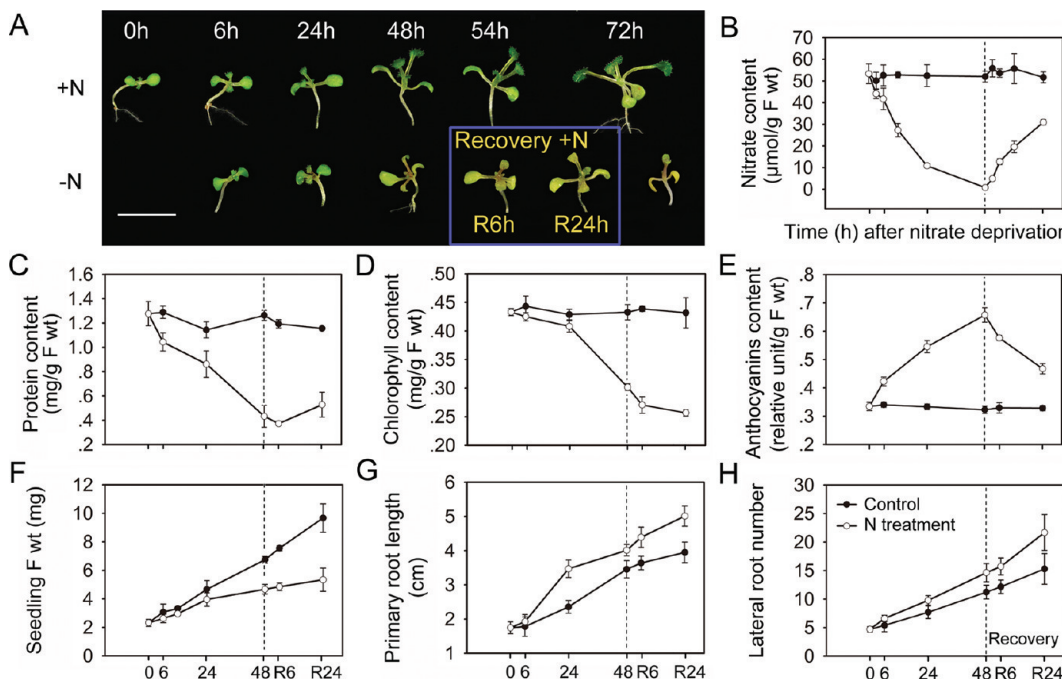


**Figure 1.** Phenotypic and physiological changes of *Arabidopsis* seedlings during nitrate deprivation. Seedlings were first grown in N-replete medium for 7 d, then transferred to N-free medium for deprivation treatments (6, 24, 48, and 72 h). Nitrate refeeding was initiated by adding 5 mM nitrate after 2 d of nitrate deprivation. (A) Phenotypic changes of the shoot during nitrate deprivation and recovery. (B–H) Changes in nitrate (B), total protein (C), chlorophyll (D) and anthocyanins (E) content, as well as fresh weight (F), primary root length (G), lateral root number (H) of the seedlings. Bar = 1 cm in (A). Data on each time-point is the mean  $\pm$  SD ( $n = 5$ ).

used for Gene Ontology (GO) enrichment analysis (Supplemental Experimental Procedures (Supporting Information)). The STRING (Search Tool for the Retrieval of Interacting Genes/Proteins) database version 8.3<sup>49</sup> with default settings (evidence view with a medium confidence cutoff of 0.4) was used for evaluation of protein–protein interactions and creation of a protein association network where proteins were represented as nodes connected via lines whose thickness represent the confidence level (0.4–0.9). In cellular localization analysis, the web-based software SUBA (SUB-cellular location database for *Arabidopsis* proteins) version 2.21<sup>50</sup> was used. For each protein, the localization with at least two evidence was considered to be significant.

#### Statistical Analysis

Unless stated otherwise, all experimental data were expressed as mean  $\pm$  standard deviation of at least 3 independent biological replicates. Statistical significances were evaluated by paired Student's *t*-test using GraphPAD Prism version 5.01 (GraphPAD Software, San Diego, CA) or SigmaPlot version 10.0 (Systat Software, San Jose, CA).

## RESULTS

### Physiological Consequences of Nitrate Deprivation in *Arabidopsis*

To understand the physiological consequences of nitrate deprivation and define a meaningful nitrate treatment regime for proteomic analyses, hydroponically cultured *Arabidopsis* (ecotype Col-0) plants were first examined for their phenotypic and physiological responses during nitrate deprivation and recovery. Plants were grown under continuous light to minimize diurnal changes in C and N metabolism, and a low shaking velocity (90 rpm) were used to provide aeration to roots and keep the shoots growing above the nutrient solution. After seedlings were grown in full N (+N) media (with 5 mM nitrate) for 7 days, they were divided into two groups: one

group remained in full N condition as the +N control, and the other group was shifted to N-free (−N) media for N deprivation treatment (Figure 1A). As shown in Figure 1B, the nitrate deprivation treatment caused rapid depletion of nitrate in plants, which was nearly undetectable ( $0.78 \pm 0.33 \mu\text{mol/g F wt}$ ) at the 48 h of deprivation. By contrast, the nitrate content remained unchanged in the N-replete seedlings. In response to this rapid decline of nitrate content in N-deprived plants, plant growth and development changed significantly as revealed by the phenotypic and physiological analyses. For example, after 2 days' N deprivation, the N-starved seedlings exhibited typical N-deficient phenotypes, including reduced total protein (Figure 1C), chlorophyll (Figure 1D), and fresh weight (Figure 1F); increased accumulation of anthocyanins in shoot (Figure 1E); and increased primary root length (Figure 1G) and lateral root number (Figure 1H). Because of the significant changes in nitrate content and other physiological parameters observed in 48 h-deprived plants, we chose this time point as the starting point for N recovery treatment (refeeding of 5 mM KNO<sub>3</sub>). Nitrate refeeding in the media gave rise to rapid recovery in contents of nitrate (Figure 1B) and total protein (Figure 1C). Anthocyanin content decreased during recovery (Figure 1E). Chlorophyll level continued to decrease within the 24 h recovery period, but the decline rate was much slower than that in the N deprivation process (Figure 1D), indicating the slow recovery of chloroplasts and photosynthesis.

### 2-DE Analysis and Identification of Nitrate-Responsive Proteins

A comparative proteomic analysis during N deprivation and refeeding was conducted to explore the mechanisms of plant response to nitrate availability. Since the nitrate signaling was believed to be a systemic process in plants,<sup>7,8</sup> the whole *Arabidopsis* seedlings were used for protein preparation and detection of whole proteome responses to nitrate deprivation. In our experiments, a typical

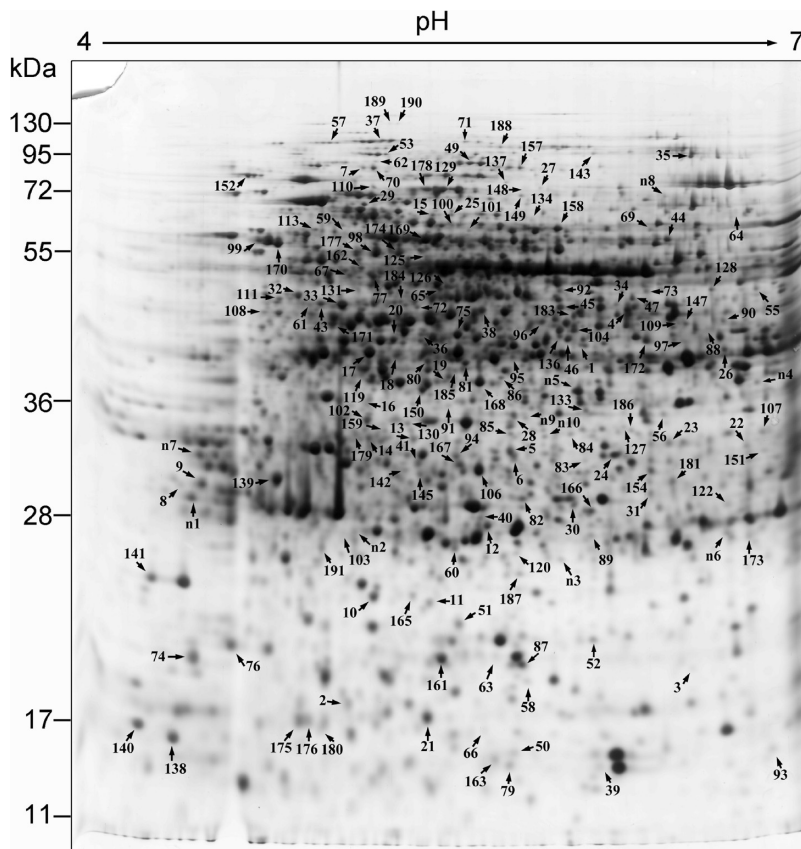


**Figure 2.** A representative 2-DE map of *Arabidopsis* proteome revealed by silver staining. Equal amount (125 µg) of total proteins from different samples were separated by 2-DE followed by silver staining. Abundance changed protein spots during nitrate deprivation and recovery were labeled by arrowheads and their detailed information was listed in Supplemental Table 2. The whole set of silver-stained gel images were shown in Supplemental Figure 1A–J.

silver-stained 2-DE gel image (Figure 2, Supplemental Figure 1A–J) contained  $2157 \pm 65$  protein spots. A total of 167 spots showed differential abundance changes by more than 1.5-fold at more than one time points, and were analyzed by MALDI-TOF/TOF MS. Of these, 157 spots were successfully determined with protein IDs (Figure 2, Supplemental Table 2, and Supplemental Spectra 1). For CBB-stained gels,  $1220 \pm 45$  spots/gel can be visualized (CBB gel in Figure 5A, Supplemental Figures 1K–M), and there were 81 abundance-changed proteins overlapped with those from the silver staining analysis. Thirteen spots only showed clear differential abundance changes on the CBB-stained gels and thus were successfully identified by MS (Figure 5A, labeled by arrowheads on CBB gel, Supplemental Table 2, and Supplemental Spectra 1). Taken together, by using two different staining methods, totally 170 protein spots with significant abundance changes during nitrate deprivation and/or recovery were identified and these 170 spots represent 137 unique proteins. 2-DE maps stained with the Pro-Q diamond dye (ProQ gel in Figure 5A, Supplemental Figure 1N–P) resolved  $736 \pm 36$  protein spots, 38 of which showed differential phosphorylation changes ( $\geq 1.5$ -fold) and 6 of them showed significant abundance changes after revisualization by CBB staining (CBB gel in Figure 5A, Supplemental Table 3, and Supplemental Spectra 2). These 38 spots represent 36 unique phosphoproteins.

Interestingly, we found some proteins that were resolved into multiple spots but shared similar up- or down-regulated accumulation patterns. We consider this could be the result of multiple isoforms, proteolytic processing, or changes in charge state caused by post-translational modifications (PTMs). For example, on the ProQ-stained gels, several proteins including

the PS II chlorophyll a/b binding protein LHCBI.2 (spots P1, P3) and LHCBI.4 (spots P2, P5) (Figure 5B, labeled by arrowheads), displayed horizontal spot shifting, presumably due to multisite phosphorylation of the proteins. The existence of multiforms of these proteins signifies their importance in plant nitrate responses as they allow plants to make fast rearrangement in metabolism and nutrient reallocation.

#### Abundance Changes and Functional Classification of the Nitrate-Responsive Proteins

The large data set of the quantitative proteome makes it difficult to discuss the identified proteins individually. To achieve a comprehensive overview of the temporal changes of the co-expressed proteins during nitrate deprivation and recovery, we used the clustering algorithm CAST to analyze the quantitative proteomic data, in which proteins with similar accumulation patterns were grouped together. As presented in Figure 3, the 170 nitrate-responsive proteins were divided into two distinct cluster groups A and B (Figure 3A). The group A includes 70 proteins (Figure 3A, Supplemental Table 4) which were up-regulated during nitrate deprivation and down-regulated after nitrate refeeding. The group B includes 100 proteins (Figure 3A, Supplemental Table 4) and has the opposite accumulation patterns to group A, namely, down-regulated during nitrate deprivation and up-regulated after nitrate refeeding. A tight correlation between seedling nitrate contents (Figure 1B) and protein abundance changes was apparently seen in the heat map (Figure 3A). For instance, 6 h of N starvation affected the abundance of only 7 proteins, while 123 and 88

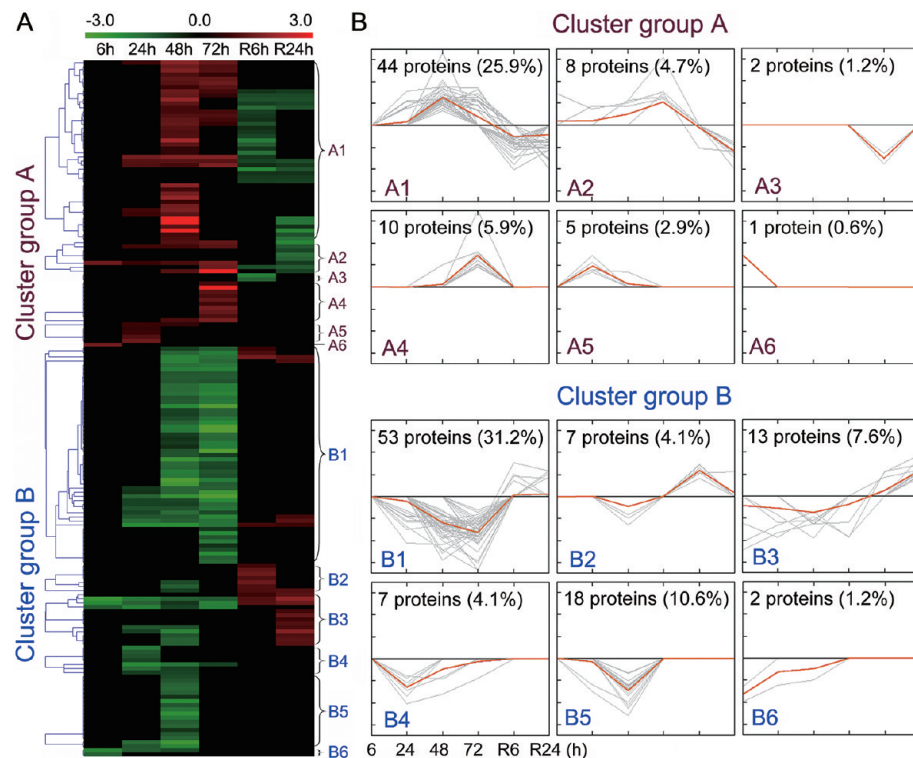


**Figure 3.** Clustering of accumulation profiles of nitrate responsive proteins in *Arabidopsis*. (A) By CAST analysis, the 170 abundance changed proteins were clustered into cluster groups A and B, each with 6 subclusters (A1–A6 and B1–B6). The CAST cluster tree was shown on the left of the heatmap and the detailed protein information in each cluster was listed in Supplemental Table 4. (B) Accumulation patterns of these 170 proteins. In each cluster, both individual (gray) and mean (orange) accumulation profiles were shown. The cluster number was shown in the lower left corner, and the number of proteins present and their percentages in total proteins were given in the upper left corner.

proteins were identified with abundance changes under 48 and 72 h of nitrate deprivation, respectively.

Cluster group A and B each contains 6 subclusters (Figure 3B, Supplemental Table 4). Accumulation profiles of individual proteins (gray lines) and their average profile (orange lines) in each subcluster were plotted in Figure 3B. For group A, the two subclusters A1 and A2 were found to be dominated by proteins involved in cell structure, stress response, proteolysis, and metabolism (Supplemental Tables 2 and 4). The subcluster A3 contains two proteins that were down-regulated after nitrate refeeding; they are the structural maintenance of chromosomes protein 2 (SMC2, spot 134) and universal stress family protein PHOS32 (spot 127). Their down-regulation indicates the alleviation of possible chromosome degradation and cellular stress induced by nitrate deprivation. Cluster A4 contains proteins mostly up-regulated at 72 h of nitrate deprivation, which are mainly involved in cellular antioxidant reactions and stress responses. These results suggest that the 72 h N-starved plants were undergoing more severe stress perturbations than 48 h-starved plants. The other two subclusters (A5, A6) contain proteins that were up-regulated during early stages (6 and 24 h) of nitrate deprivation including L-ascorbate peroxidase 1 (APX1, spot 31), glutamine synthetase 1 (GS1, spot 18), and 26S proteasome AAA-ATPase subunit RPT5a (spot 32), indicating that cell redox status, N remobilization, and 26S proteasome-mediated protein degradation are very sensitive to plant N status changes.

In cluster group B, the subcluster B1 contains 53 proteins and most of them were gradually down-regulated, with the largest decrease at 72 h of nitrate deprivation. Proteins in this cluster are mostly chloroplast components (Supplemental

Tables 2 and 4) such as Rubisco large subunits (spots 10, 92, and 166) and small subunits (spots 50, 93, and 163), and so forth. Their down-regulation indicates that the photosynthetic apparatus was undergoing extensive degradation under nitrate deprivation. After nitrate refeeding, these proteins showed little recovery. This result explains why the chlorophyll content in shoots remained decreased after nitrate refeeding (Figure 1D) and suggests that the refoundation of chloroplasts in plant recovery from nitrate deprivation is a relatively slow process. Proteins in subclusters B2 and B3 had a pattern of down-regulation under nitrate deprivation and up-regulation after nitrate refeeding. The involvement of the nitrite reductase 1 (NiR1, spots 69 and 158) in these subclusters represents one of the typical primary nitrate responses.<sup>12,23</sup> Other proteins from these two subclusters include proteins involved in amino acids and protein biosynthesis such as the 60S acidic ribosomal protein P2 (PP2A, spot 140; PP2B, spot 138) and translation initiation factor 3 (eIF-3, spot 149). Several proteins with regulatory functions such as Ca<sup>2+</sup> signaling component annexin *Arabidopsis* 2 (spot 133), TIM-barrel signal transduction protein (spot 137), and nuclear DNA-binding protein G2p (spot 128) were also found here, suggesting a complex regulatory network of plant nitrate responses. Last three subclusters B4, B5, and B6 contained mostly chloroplast components with accumulation pattern similar to subcluster B1 (Supplemental Tables 2 and 4). Other proteins in this subcluster include those related to protein metabolism and carbohydrate metabolism (Supplemental Tables 2 and 4).

To compare protein functional distributions between the two cluster groups (A and B), GO enrichment analysis was carried out using the 70 proteins in group A and 100 proteins in groups

B, respectively, with three sets of ontologies: biological process (GOBP), molecular function (GOMF), and cellular component (GOCC). As shown in Figure 4, in GOBP enrichment

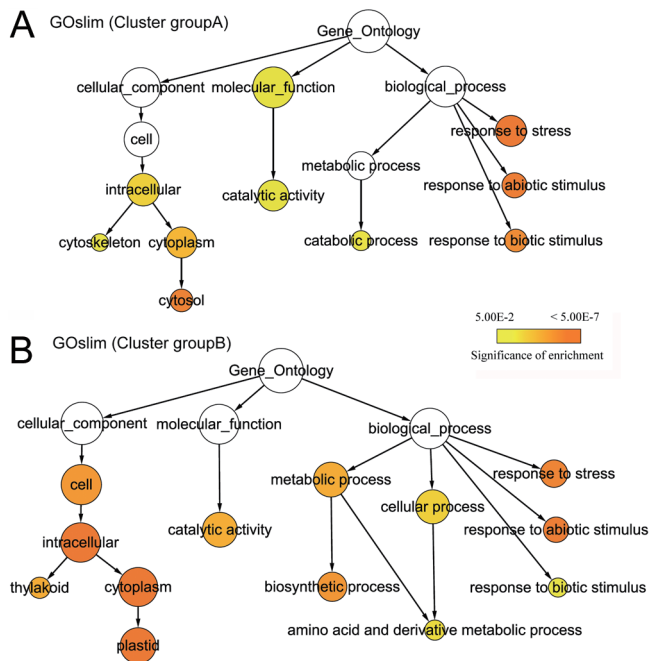


**Figure 4.** Enrichment of Gene Ontology annotations for abundance changed proteins in the CAST cluster groups. Using Bingo plugin in Cytoscape, enrichment of GO annotations was computed for cluster groups A (A) and B (B), respectively (70 proteins in group A; 100 proteins in group B). Over-represented terms were displayed graphically as yFiles hierarchical trees for three GO vocabularies (GOBP, GOMF, and GOCC). The size of the node is proportional to the number of molecules within this group, and the color of the node represents the significance of enrichment (see the color scale).

analysis, nitrate deprivation strongly induced the accumulation of stress-responsive proteins such as redox proteins in group A, and to a less significance, proteins in catabolic processes such as proteases. Similarly, in group B, stress-responsive proteins remain highly enriched, but there are more proteins with an association with metabolic and cellular processes, particularly those in biosynthetic processes. The repression of these processes under nitrate deprivation could minimize consumption of the limited N resource. For GOMF enrichment, the catalytic activity was the main function as a large number of enzymes were identified in both groups A and B. For GOCC enrichment, proteins in group A were mostly cytoplasm-localized, while proteins in group B localized mostly in plastids.

#### Nitrate Deprivation-Induced Protein Phosphorylation Changes

To verify that some of the nitrate-responsive proteins are indeed regulated by post-translational mechanisms such as protein phosphorylation, 2-DE gels of the nitrate deprivation and recovery samples were stained with the ProQ Diamond dye to gain a proteome-wide understanding of protein phosphorylation changes during plant nitrate responses. This method is based on the principle that ProQ dye binds specifically to the phosphate moiety of phosphoproteins with high sensitivity and linearity.<sup>42</sup> Under the stringent gel analysis conditions, spots with low staining quality such as overlapping, smearing, and severe distorting were excluded to avoid contamination by nonphosphorylated proteins. From this

analysis, we identified 38 protein spots (representing 36 unique proteins) that have significant phosphorylation changes ( $\geq 1.5$ -fold), as assessed by changes in spot fluorescence intensity (ProQ gel in Figure 5A, Supplemental Table 3). Functional classification revealed that diverse biological processes particularly the fundamental metabolic pathways were regulated by protein phosphorylation during plant responses to variable nitrate levels (Supplemental Table 3). Among these, 28 spots showed changes after 48 h of nitrate deprivation and 20 spots after 24 h of nitrate refeeding, with 10 spots shared by both treatments. Among the 28 spots from 48 h of nitrate deprivation, 12 proteins were highly phosphorylated and 16 were dephosphorylated. In 24 h N-recovered samples (R24h), 7 proteins showed increased phosphorylation, and 13 reduced phosphorylation. These data suggest active involvement of protein phosphorylation in plant responses to N deficiency.

To verify that the nitrate-responsive phosphoproteins we identified are real, we first delivered the same reconstituted tryptic peptides of 2DE gel spots previously used for protein identification to a LTQ mass spectrometer. However, after repeated attempts, we did not detect any phosphopeptides in these samples, probably due to the low abundance of phosphopeptides eluted from the gel spots. We then applied a MS-based phosphoproteomic study to map the phosphorylation sites of the 38 phosphoproteins we identified using the total proteins from the 48 h N-starved, 48 h N-replete, and 24 h recovered seedlings, respectively. The phosphopeptides were enriched by Ti<sup>4+</sup>-IMAC microspheres before they were delivered to the LTQ mass spectrometer for phosphorylation site mapping. Using this method, 20 out of the 38 phosphoproteins identified by the Pro-Q staining (representing 18 unique proteins) were reidentified with one or more phosphopeptides (Supplemental Table 5 and Supplemental Spectra 3). In addition, we searched our phosphoproteins against the *Arabidopsis* protein phosphorylation site database (PhosPhAt version 3.0)<sup>51</sup> and found that 61% of them (labeled with asterisks after the spot numbers in Supplemental Table 3) were previously experimentally identified phosphoproteins. These results partially validated the phosphoprotein identification from ProQ staining and approved the effectiveness of phosphoprotein identification by ProQ staining.

To further determine the abundance changes of the identified phosphoproteins, the ProQ-stained 2-DE gels were restained with CBB staining. Only 6 protein spots were found to have significant abundance changes on CBB-stained gels (CBB gel in Figure 5A, Supplemental Table 3), which include LHCBl.2 (spots P1, P3), RCA (spot P6), and CARB (Carbamoyl phosphate synthetase large chain, spot P26). The significant changes in both abundance and phosphorylation state of these 6 proteins (Figure 5) suggest that they play important roles in plant nitrate responses.

#### Functional Validation of the Identified Nitrate-Responsive Proteins

To functionally validate the nitrate-regulated proteins identified in this study, several proteins (three from cluster group A, four from cluster group B) were selected to test their involvement in plant nitrate responses by using T-DNA insertion mutants and/or overexpression transgenic lines of their coding genes. Plants were grown on 1/2 MS-N agar plates for nitrate deprivation and observed for nitrate-responsive growth phenotypes. From these studies, we found that the 26S proteasome regulatory subunit RPT5a regulates plant N use efficiency, and the cytoskeleton protein TUA6 has a role in regulating anthocyanin accumulation

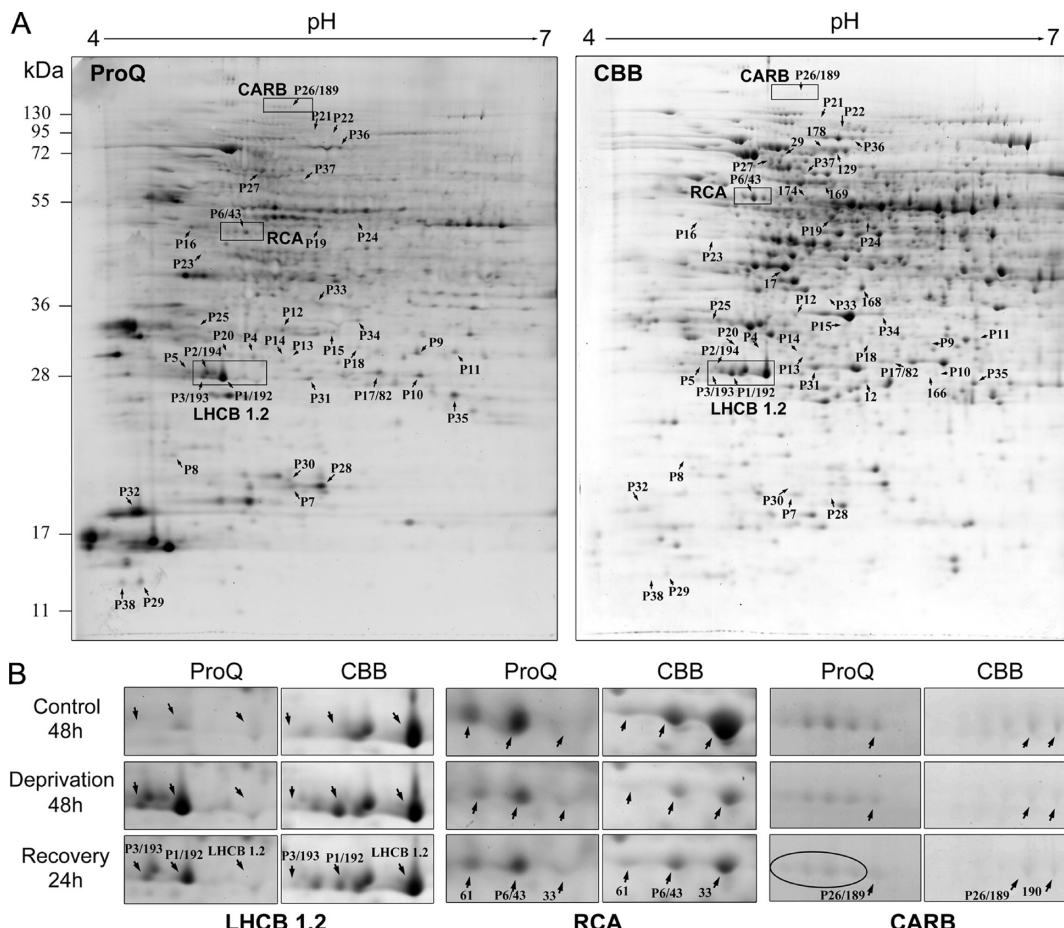


**Figure 5.** 2-DE maps of protein spots revealed by ProQ and CBB staining. (A) Equal amount (800 µg) of total proteins were separated by 2-DE followed by ProQ (left) and CBB (right) staining. The 38 protein spots showing phosphorylation level changes during nitrate deprivation and recovery were labeled by arrowheads on the ProQ map and their detailed information was listed in Supplemental Table 3. The proteins with abundance changes were labeled by arrowhead on the CBB map. (B) The proteins showing multiple phosphorylation changes were indicated by rectangular frames, which include the light harvesting chlorophyll a/b binding protein (LHCb1.2), Rubisco activase (RCA), and Carbamoyl phosphate synthetase large chain (CARB). The complete set of CBB and ProQ stained gel images were shown in Supplemental Figure 1K–P.

in plants. No apparent growth phenotypes were found in the lines for other proteins under nitrate deprivation conditions, suggesting they might be involved in plant N responses other than growth regulation or anthocyanin biosynthesis.

From the experiments with T-DNA insertional mutants, we observed that two T-DNA mutant alleles of the 26S proteasome regulatory subunit RPT5a, *rpt5a-2* and *rpt5a-3*, grew much greener on –N medium compared to their wild-type (WT) plants (Figure 6A). Under normal +N conditions, *rpt5a-2* mutant is a semi-dwarf with apparent repression of the root growth. These phenotypes were even stronger in the *rpt5a-3* mutant. During nitrate deprivation, both mutants and the WT showed increased root growth and decreased shoot protein and chlorophyll contents, but the changes in the WT were much greater (Figure 6). By the 13th day of nitrate deprivation, the mutants developed more new leaves than the WT (Figure 6A). These results indicate that the loss of function of the *RPT5a* reduced plant sensitivity to low nitrate stress, and suggest that RPT5a is a negative regulator of nitrate-dependent plant photomorphogenesis.

To determine whether the reduced sensitivity of the *rpt5a* mutants are specific to plant response to low nitrate stress, we tested their responses to other stress conditions including phosphorus and potassium deprivation, salinity (NaCl), and mannitol-induced osmotic stress (for detailed experimental

procedures, see Supporting Information). As expected, we did not observe a significant difference between the WT and mutants in response to these stress conditions (Supplemental Figures 2A–C), suggesting that RPT5a specifically regulates plant nitrate responses.

To further characterize the functions of RPT5a, we grew the *rpt5a-3* mutant in soil with full nutrients for 50 days, in three batches. As described previously,<sup>35</sup> the *rpt5a-3* showed severe semi-dwarf phenotype with much smaller shoot and root systems, compared to the WT (Figure 7A). The mutant plants had similar size of siliques as compared with the WT (Figure 7B), but the biomass ratio of siliques to shoots in the mutant was about 20% higher than that of the WT (Figure 7C). This interesting result implies a greater yield potential and higher N remobilization efficiency when the *RPT5a* gene is down-regulated.

From the gene overexpression analyses, we observed that one transgenic line (CS6551, from the ABRC Stock Center) overexpressing the *Tubulin subunits alpha-6 (TUA6)* gene fused to GFP (35S::GFP-TUA6) accumulates more anthocyanins under the low N (1 mM nitrate) condition. As shown in Figure 8A,B, after growing for 15 days on the control media (6 mM nitrate), the transgenic line showed slightly smaller rosette compared to the WT control, and both had very low anthocyanin accumulation. When grown on low N (1 mM nitrate) plates, both

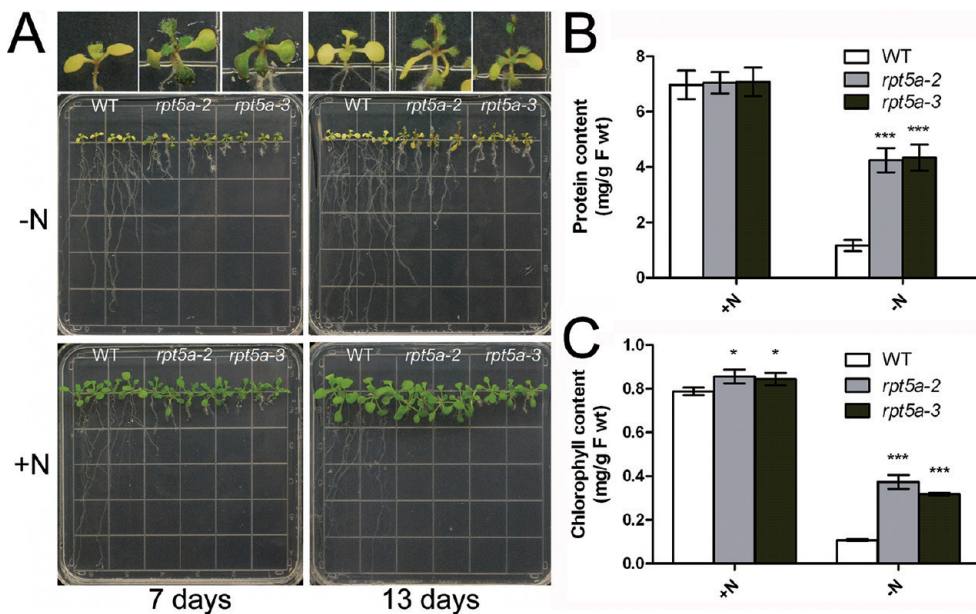


**Figure 6.** Characterization of mutants for the 26S proteasome regulatory subunit RPT5a under nitrate deprivation. (A) Phenotypes of the WT plants and *rpt5a-2*, *rpt5a-3* mutants grown under nitrate deprivation. Seedlings were first grown on 1/2 MS medium for 6 d, then transferred onto +N (with 6 mM KNO<sub>3</sub>) or -N (6 mM KNO<sub>3</sub> was replaced with 6 mM KCl) medium to grow for additional 13 days. A close-up image of the shoot of each genotype was shown on the top of the corresponding seedlings. (B and C) Changes in shoot protein (B) and chlorophyll (C) contents in the WT and mutants measured after 13 days of nitrate deprivation. Data are the mean  $\pm$  SD ( $n = 3$ ). Asterisks (\* and \*\*): Significance of differences according to *t*-test ( $*p < 0.05$  or  $***p < 0.001$ ).

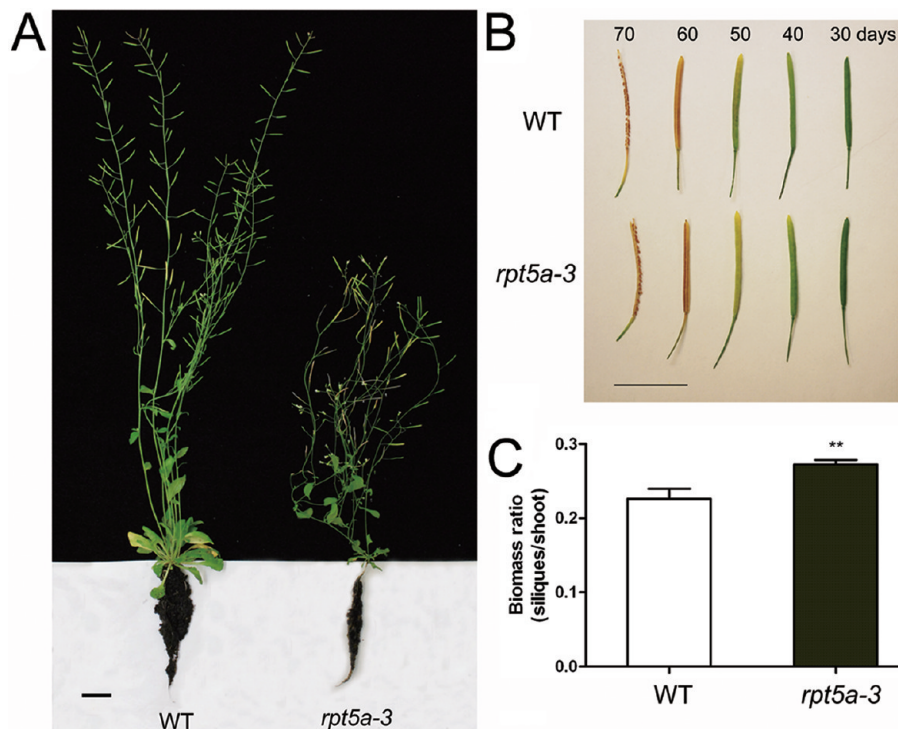


**Figure 7.** The *rpt5a-3* mutant showed enhanced N use efficiency during reproductive growth. (A) Growth phenotypes of the 50-day-old *rpt5a-3* and WT plants grown in soil. (B) Siliques phenotypes of the WT and mutant plants at deferent growth stages (30, 40, 50, 60, and 70 d). (C) Difference in biomass ratios of the siliques to shoot per plant between *rpt5a-3* and WT. Bar = 2 cm in (A), 1 cm in (B). Data are the mean  $\pm$  SD ( $n = 3$ ). Asterisks (\*\*): Significance of differences according to *t*-test ( $p < 0.01$ ).

WT and the transgenic plants showed typical N deficiency phenotypes including decreased chlorophyll accumulation and reduced shoot/root ratio. The most significant difference between them was that the transgenic plants accumulated more

anthocyanins (Figure 8A–C). To examine whether the high anthocyanin accumulation in the transgenic plants is due to the accumulation of the TUA6 protein, the steady-state level of the GFP-TUA6 fusion protein in the shoots and roots were assessed

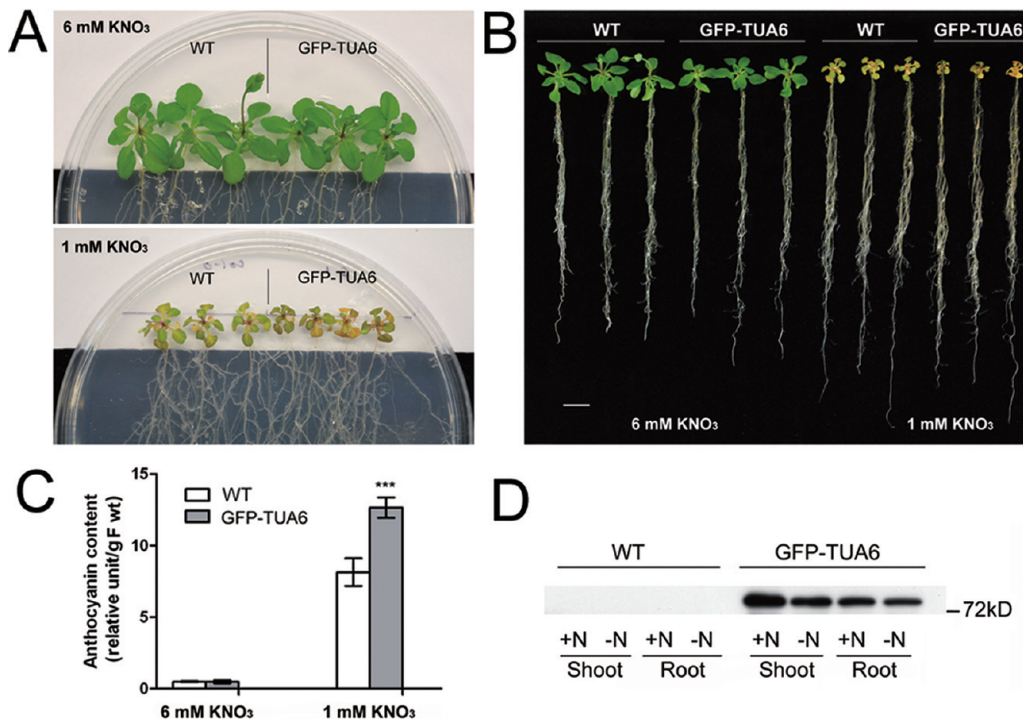


**Figure 8.** TUA6 overexpression plants accumulate more anthocyanins in shoots under low N conditions. (A and B) Shoot and root phenotypes of WT and the 35S::TUA6-GFP overexpression plants under nitrate deprivation. Seedlings were first grown on 1/2 MS medium for 6 d, then transferred onto low N medium (with 1 mM KNO<sub>3</sub>, 5 mM KCl) or high N medium (with 6 mM KNO<sub>3</sub>) for 15 days. (C) Anthocyanin contents in shoots of the WT and overexpression plants grown under low N or high N for 15 d. (D) Western blot analysis of GFP-TUA6 protein levels in shoots and roots of the WT (Col-0) and 35S::TUA6-GFP plants under high N (6 mM KNO<sub>3</sub>) and low N (1 mM KNO<sub>3</sub>) conditions. Equal amount (10 µg) of total proteins from different plants and treatments were loaded on the same gel for Western blotting. GFP-TUA6 protein levels were detected by an anti-GFP antibody. Bar = 1 cm. Data are the mean ± SD ( $n = 5$ ). Asterisks (\*\*\*): Significance of difference according to *t*-test ( $p < 0.001$ ).

before and after nitrate deprivation by Western blot analysis using an anti-GFP antibody (Supplemental Experimental Procedures in Supporting Information). Surprisingly, we found that the GFP-TUA6 protein level in the transgenic plants was greatly down-regulated by N starvation in the shoots but not in the roots (Figure 8D), indicating that active PTM-regulated TUA6 degradation was occurring in the shoot tissues. These results also suggest that the TUA6 protein is negatively correlated with the low nitrate-induced anthocyanin accumulation in plants.

## ■ DISCUSSION

### Reprogramming of Plant Metabolisms during Nitrate Deprivation

In this study, we carried out a comprehensive proteomic study on plant nitrate responses by using 2-DE with three different staining methods, coupled with the MALDI TOF/TOF mass spectrometry. As a result, a total of 170 and 38 proteins were found to have abundance and phosphorylation state changes, respectively, in response to nitrate deprivation and subsequent recovery. Bioinformatics analyses of these nitrate-responsive proteins (Figures 3 and 4) revealed that under nitrate deprivation conditions, the most significant changes are: (i) impairment of N and C assimilation, photosynthesis, and protein synthesis machineries; and (ii) activation of cytoskeleton, N remobilization, protein degradation, and antioxidant systems. Among these changes, the last three processes (N remobilization, protein degradation, and antioxidant systems) changed very early (6 h) in response to N starvation, suggesting that they represent early processes of plant nitrate responses. After nitrate refeeding, N metabolism, photosynthesis, and protein

synthesis were gradually recovered, whereas proteins involved in protein degradation and cytoskeleton were down-regulated. It is intriguing that proteins in the antioxidant systems showed little changes during the 24 h recovery process, suggesting that a high level of antioxidation activity may be essential for plants to recover from the low N stress. The over-representation of proteins in these processes reflected a major metabolic rearrangement during plant adaptation to altered nitrate availability.

### Remodeling of Plant C/N Balance under Nitrate Deprivation

In higher plants, after being transported into the cytoplasm by nitrate transporters, nitrate is reduced to nitrite by nitrate reductase (NR), and then translocated into the plastid for reduction to ammonium by nitrite reductase (NiR).<sup>3</sup> The ammonium is primarily assimilated in the plastid by the GS/GOGAT cycle.<sup>3</sup> Alternatively, ammonium can be incorporated into carbamoyl phosphate by carbamoyl phosphate synthase (CARB or CPSase) in plastid and the carbamoyl phosphate can be further transformed into arginine by the urea cycle<sup>52</sup> (Supplemental Figure 3). In our study, perhaps due to the relatively narrow pH range (4–7) of the DryStrips used in 2DE, we did not pick up any nitrate transporters, which are generally hydrophobic membrane proteins with high isoelectric points (generally >10).<sup>4</sup> However, after 48 h of nitrate deprivation, the abundance of several N assimilation-related enzymes such as NiR (spots 69, 158), CARB (spots 189, 190, P26), arginosuccinate synthase (ASS, spot 126), and carbonic anhydrase (CA2, spot 41) was clearly down-regulated (Supplemental Figure 3). After nitrate refeeding, the abundance of NiR and ASS quickly increased, indicating that nitrate assimilation via

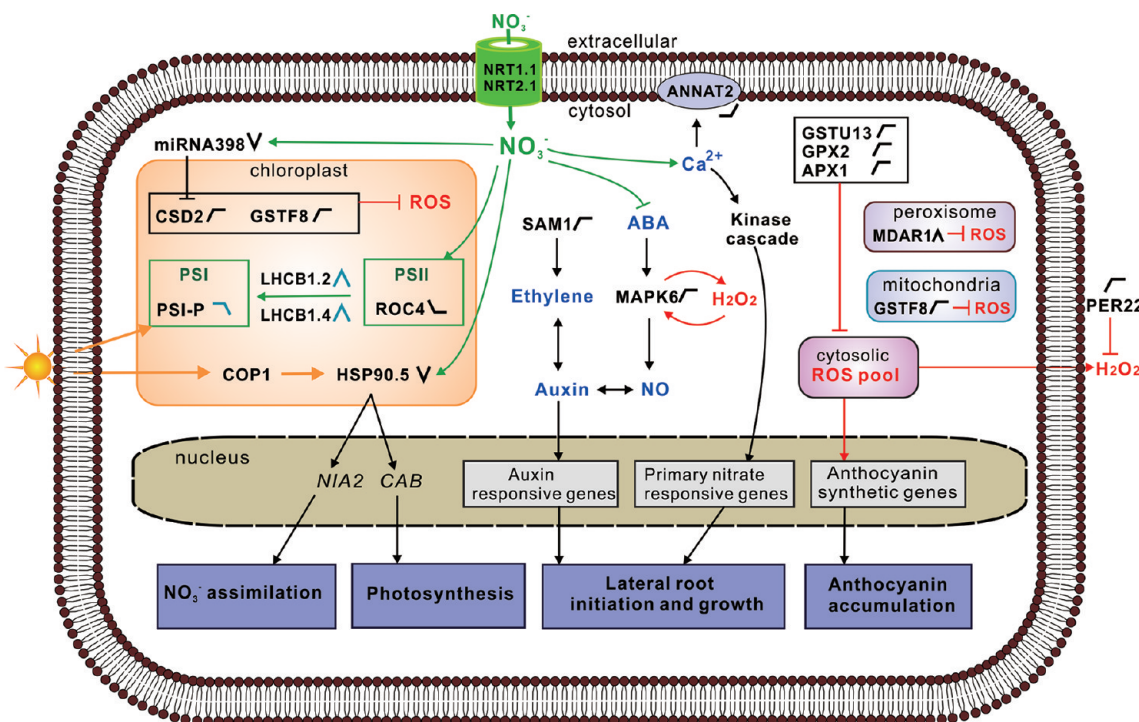


**Figure 9.** A model for regulatory networks of plant nitrate responses. For simplicity, all regulators are presented in the same cell, although it may not be the case in real situations. Arrows indicate positive regulations, and bars mean negative regulations. Green lines represent nitrate signaling pathways, red lines show ROS signaling pathways, and orange lines indicate light signaling. Each regulator is followed by a curve for abundance (black curve) or phosphorylation state (blue curve) changes during nitrate deprivation and recovery. Upward lines indicate increased phosphorylation, while downward lines indicate decreased phosphorylation (or dephosphorylation). Horizontal lines mean no changes. *NIA2*, gene encoding for the nitrate reductase 2; *CAB*, gene for chlorophyll binding proteins. Other abbreviations were explained in Supplemental Tables 2 and 3.

both GS/GOGAT and urea cycle was affected by altered nitrate availability.

C and N metabolisms are interconnected in plants and a C/N balance is crucial for optimal growth and development of plants.<sup>10</sup> Therefore, it is not surprising that in our proteomic study, C metabolism-related processes such as photosynthesis, pentose phosphate pathway, and glycolysis were significantly affected by nitrate deprivation (Supplemental Tables 2 and 3). Consistently, the C/N metabolisms and energy pathways were also enriched in the protein interaction network analysis (the STRING analysis) (Supplemental Figure 4), which also suggests a remodeling of plant C/N balance during nitrate deprivation and refeeding. Thiamine pyrophosphate (TPP) is the cofactor of transketolase in pentose phosphate pathway and the synthesis of its precursor thiamine (vitamin B1) is catalyzed by thiazole biosynthetic enzyme THI1 (spot 5).<sup>53</sup> Since THI1 abundance decreased significantly at as early as 6 h of nitrate deprivation and increased quickly after 6 h of nitrate refeeding, we infer that THI1 is a key factor in regulating plant C and N balance.

#### Enhanced Protein Degradation through the 26S Proteasome Pathway under Nitrate Deprivation

In this study, more than 60 of the identified proteins were related to amino acid metabolism, RNA processing, protein synthesis, folding, transport, and proteolysis, indicating that protein and amino acid metabolisms were the most significantly affected biological processes in plant nitrate responses (Supplemental Tables 2 and 3 and Supplemental Figure 4). From our data set, intensive protein degradation was seen under nitrate deprivation as revealed by the enrichment of proteins involved in proteolysis (Figure 3C, cluster group A). Among these are five proteins from

the ubiquitin/26S proteasome machinery, including PAA2 (spot 160), PAB2 (spot 40), PBA1 (spot 120) in the 20S core particle and RPT1A (spot 73), RPT5a (spot 32) in the 19S regulatory particle which were all up-regulated during nitrate deprivation. A previous genetic study has implicated NLA, a RING-type ubiquitin E3 ligase in plant adaptation to nitrate limitation in *Arabidopsis*.<sup>26</sup> In this study, we identified more proteins from the 26S proteome pathway that regulate plant nitrate responses. Further functional studies on genes indicated that the RPT5a plays a role in modulating plant NUE and N remobilization at the reproductive stage as the *RPT5a* loss-of-function mutants had a higher silique/shoot ratio (Figure 7) and accumulated more protein and chlorophyll in the shoots as compared with the WT (Figure 6). Furthermore, the semi-dwarf phenotypes of the *rpt5a* mutants suggest that RPT5a is essential for plant shoot and root development, although the underlying mechanisms remain to be understood.

#### Regulatory Networks of Plant Nitrate Responses Revealed by the Proteomic Data

Although previous microarray, gene function, and systems biology studies have unraveled a number of genes and factors that have potential regulatory roles in plant N metabolism and signaling in *Arabidopsis*, the whole picture of plant N or nitrate signaling network remains very elusive. By employing a comprehensive proteomic analysis in this study, we identified more than 200 proteins whose abundance and/or phosphorylation state were directly regulated by N status changes. These proteins provided novel evidence for plant N responses at the protein level and brought insights into their interactions with other signaling pathways (such as ROS, phytohormones, Ca<sup>2+</sup> and light, etc.). On the basis of our proteomic data and other

published results in literature, we proposed a model for the regulatory networks of plant nitrate responses (Figure 9). Briefly, plasma membrane-localized nitrate transporters NRT1.1, and probably NRT2.1, sense changes in extracellular nitrate concentrations and transduce the nitrate signal inside the cell by connecting with other pathways such as ROS, ethylene, auxin, ABA,  $\text{Ca}^{2+}$  and light signaling as elaborated below.

- (i) Connection with ROS signaling. It is well-known that under N limiting conditions, overaccumulation of reducing equivalents and elevated lipid degradation can promote the generation of ROS.<sup>54</sup> To avoid the oxidative damage, plants need to activate the ROS-scavenging pathways to destroy the excess ROS. In line with this assumption, a number of antioxidative enzymes were up-regulated during nitrate deprivation, including CSD2 (spot 51), GSTF8 (spot 173) in chloroplasts, GPX2 (spot 165), APX1 (spot 31), GSTU13 (spot 12) in cytosol, GSTF8 (spot 173) in mitochondrion, MDAR1 (spot 90) in peroxisome, and PER22 (spot 172) in the extracellular fraction (Supplemental Table 6). As part of plant antioxidative system, the anthocyanin synthetic genes are also under ROS regulation.<sup>55</sup> In addition, there was evidence showing that nitrate can induce the expression of *Arabidopsis* miR398<sup>25</sup> and miR398 can repress the translation of the copper/zinc superoxide dismutase 2 (CSD2),<sup>56</sup> suggesting that the nitrate signaling can regulate plant ROS status via miRNA(s) at the transcriptional level.
- (ii) Connection with phytohormone signaling. It is interesting to point out that in this study, out of the three SAM proteins identified for S-adenosylmethionine synthesis, only SAM1 showed up-regulation under nitrate deprivation. SAM1 was reported to be the only SAM protein involved in ethylene synthesis<sup>57</sup> and ethylene can induce primary root growth by regulating auxin biosynthesis and translocation.<sup>58</sup> Therefore, the up-regulation of SAM1 may support the involvement of ethylene signaling in enhancing root growth under nitrate deprivation (Figure 1G,H). ABA is known to be able to promote NO and  $\text{H}_2\text{O}_2$  production by enhancing the accumulation of mitogen-activated protein kinase 6 (MAPK6),<sup>59,60</sup> while the NO produced may interact with auxin to promote the development of lateral root.<sup>61</sup> Therefore, the result of up-regulation of MAPK6 (spot72) under nitrate deprivation in this study is consistent with a previous finding that ABA signaling was repressed by nitrate.<sup>62</sup>
- (iii) Connection with  $\text{Ca}^{2+}$  signaling. Annexins are  $\text{Ca}^{2+}$ -dependent membrane-binding proteins and important components of  $\text{Ca}^{2+}$  signaling pathways.<sup>63</sup> The up-regulation of an annexin 2 (ANNAT2, spot 133) during nitrate recovery in this study confirmed the involvement of  $\text{Ca}^{2+}$  signaling in plant nitrate responses. Meanwhile,  $\text{Ca}^{2+}$  can enhance primary nitrate response by activating a kinase cascade,<sup>21</sup> which further highlights the importance of  $\text{Ca}^{2+}$  signaling in plant nitrate responses.
- (iv) Connection with light signaling. In chloroplasts, HSP90.5 (CR88, spot 152), which is controlled by a light signaling transducer COP1, can enhance photosynthesis and nitrate assimilation by activating the expression of nitrate reductase gene *NIA2*, and chlorophyll-binding protein gene *CAB*.<sup>64,65</sup> In this study, the repression of HSP90.5 under nitrate deprivation and activation after nitrate refeeding suggest a possible role of HSP90.5 in the crosstalk

between nitrate and light signaling. In addition, the early down-regulation (6 h of nitrate deprivation) of a chloroplast stromal cyclophilin 20-3 (ROC4, spot 3) that is involved in the repair of photodamaged PSII<sup>66</sup> also suggests an intimate relationship between nitrate and light signaling.

- (v) Connection with protein phosphorylation. Post-translational modifications provide other levels of regulation in plant nitrate responses. It is well-known that nitrate reductase (NR) and nitrate sensor NRT1.1/CHL in higher plants are regulated by phosphorylation. Recently, a phosphoproteomic study in *Arabidopsis* revealed several groups of phosphoproteins regulated by nitrate and ammonia, which include GPI-anchored proteins, receptor kinases, and transcription factors.<sup>67</sup> In this study, we identified 38 nitrate-responsive unique proteins regulated by phosphorylation in *Arabidopsis* (Supplemental Table 3). Among these are LHCBI.2 (spots P1, P3) and LHCBI.4 (spots P2, P5), two major chlorophyll-binding proteins in PSII. The phosphorylation changes of LHCBI proteins reflects the energy balance of the photosynthetic machinery.<sup>68</sup> During nitrate deprivation, both LHCBI.2 and LHCBI.4 were found to be phosphorylated, indicating a state transition from PSII to PSI. Other phosphoproteins identified include those involved in C and N metabolism, cell redox homeostasis and protein turnover (Supplemental Table 3), indicating that these processes are also subject to phosphorylation regulation under variable nitrate conditions.

## CONCLUSION

This study provides a most comprehensive proteomic analysis of plant nitrate responses to date. By using 2-DE-coupled mass spectrometry, we identified 170 proteins with abundance or phosphorylation changes in response to nitrate variation. Compared to previous nitrate related proteomic studies in plants,<sup>31–33,67</sup> this study identified more protein spots which allowed us to gain novel insights into the regulatory networks of plant nitrate responses. Further functional studies on genes using reverse genetic approaches confirmed the roles of some nitrate-responsive proteins identified. More interestingly, by adopting the ProQ diamond fluorescence staining method, we identified 38 nitrate-regulated phosphoproteins that are involved in diverse biological processes such as cell redox homeostasis, photosynthesis, protein turnover, and N metabolism. However, due to the genuine limitation associated with the ProQ staining method, the number of nitrate-regulated phosphoproteins identified in this study was still small. Thus, we are in the process of using more efficient phosphoprotein enrichment methods such as  $\text{TiO}_2$  and  $\text{Ti}^{4+}$ -IMAC to achieve more comprehensive profiling of the nitrate-regulated phosphoproteins, which is expected to be highly valuable to future studies of the N response pathways and signaling mechanisms in plants.

## ASSOCIATED CONTENT

### Supporting Information

Supplemental experimental procedures, Supplemental Table 1, Supplemental Figures 1–4 and Supplemental Spectra 1–3. Supplemental Tables 2–6 were presented in separate Excel files. This material is available free of charge via the Internet at <http://pubs.acs.org>.

## AUTHOR INFORMATION

### Corresponding Author

\*Hanfa Zou: email, hanfazou@dicp.ac.cn; phone, +86-411-84379610; fax, +86-411-84379620. Samuel Sai-Ming Sun: email, ssun@cuhk.edu.hk; phone, +852 3943 6286; fax, +852 2603-5441. Jun-Xian He: email, jxhe@cuhk.edu.hk; phone, +852 3943 1271; fax, +852 2603-6382.

### Notes

The authors declare no competing financial interest.

## ACKNOWLEDGMENTS

We thank Ms. Yu-Dong Wang and Ms. Cheng Zhang for assistance in experiments, Prof. Jean-Luc Gallois (Institut National de la Recherche Agronomique-UR1052 Station de Génétique et d'Amélioration des Fruits et Légumes, France) for kindly providing the *rptSa* mutants. This work was partially supported by the National Transgenic Project of China (No. 2009ZX08003-004b), Hong Kong RGC General Research Fund 465009 & 465410 and the Direct Grants from the Chinese University of Hong Kong (to J.-X.H.); the National Transgenic Project of China (No. 2009ZX08009-001b), the Hong Kong UGC AoE Center for Plant and Agricultural Biotechnology Project AoE-B-07/09 and a special fund from the Resource Allocation Committee, The Chinese University of Hong Kong (to S.S.-M.S.).

## ABBREVIATIONS

C, carbon; N, nitrogen; NUE, nitrogen use efficiency; MS medium, Murashige and Skoog medium; GO, Gene Ontology; PTM, post-translational modifications; WT, wild type; F wt, fresh weight; SD, standard deviation; Rubisco, Ribulose-1,5-bisphosphate carboxylase/oxygenase; PSI/II, Photosystem I/II; HSP, heat shock protein; ROS, reactive oxygen species; ABA, abscisic acid; NO, nitric oxide; TEMED, *N,N,N',N'*-tetramethyl-ethane-1,2-diamine; 2-DE, two-dimensional electrophoresis; CBB, Coomassie Brilliant Blue; LTQ, linear quadrupole ion trap

## REFERENCES

- (1) Lam, H. M.; Coschigano, K. T.; Oliveira, I. C.; Melo-Oliveira, R.; Coruzzi, G. M. The molecular-genetics of nitrogen assimilation into amino acids in higher plants. *Annu. Rev. Plant Physiol. Plant Mol. Biol.* **1996**, *47*, 569–593.
- (2) Forde, B. G. Local and long-range signaling pathways regulating plant responses to nitrate. *Annu. Rev. Plant Biol.* **2002**, *53*, 203–224.
- (3) Masclaux-Daubresse, C.; Daniel-Vedele, F.; Dechorganat, J.; Chardon, F.; Gauichon, L.; Suzuki, A. Nitrogen uptake, assimilation and remobilization in plants: challenges for sustainable and productive agriculture. *Ann. Bot.* **2010**, *105* (7), 1141–1157.
- (4) Miller, A. J.; Fan, X.; Orsel, M.; Smith, S. J.; Wells, D. M. Nitrate transport and signalling. *J. Exp. Bot.* **2007**, *58* (9), 2297–2306.
- (5) Hodge, A.; Robinson, D.; Fitter, A. Are microorganisms more effective than plants at competing for nitrogen? *Trends Plant Sci.* **2000**, *5* (7), 304–308.
- (6) Skiba, M. W.; George, T. S.; Baggs, E. M.; Daniell, T. J. Plant influence on nitrification. *Biochem. Soc. Trans.* **2011**, *39* (1), 275–278.
- (7) Castaings, L.; Marchive, C.; Meyer, C.; Krapp, A. Nitrogen signalling in *Arabidopsis*: how to obtain insights into a complex signalling network. *J. Exp. Bot.* **2011**, *62* (4), 1391–1397.
- (8) Krouk, G.; Crawford, N. M.; Coruzzi, G. M.; Tsay, Y.-F. Nitrate signalling: adaptation to fluctuating environments. *Curr. Opin. Plant Biol.* **2010**, *13* (3), 265–272.
- (9) Scheible, W.-R.; Lauerer, M.; Schulze, E.-D.; Caboche, M.; Stitt, M. Accumulation of nitrate in the shoot acts as a signal to regulate shoot-root allocation in tobacco. *Plant J.* **1997**, *11* (4), 671–691.
- (10) Gutierrez, R.; Lejay, L.; Dean, A.; Chiaromonte, F.; Shasha, D.; Coruzzi, G. Qualitative network models and genome-wide expression data define carbon/nitrogen-responsive molecular machines in *Arabidopsis*. *Genome Biol.* **2007**, *8* (1), R7.
- (11) Wang, R.; Okamoto, M.; Xing, X.; Crawford, N. M. Microarray analysis of the nitrate response in *Arabidopsis* roots and shoots reveals over 1,000 rapidly responding genes and new linkages to glucose, trehalose-6-phosphate, iron, and sulfate metabolism. *Plant Physiol.* **2003**, *132* (2), 556–567.
- (12) Scheible, W. R.; Morcuende, R.; Czechowski, T.; Fritz, C.; Osuna, D.; Palacios-Rojas, N.; Schindelasch, D.; Thimm, O.; Udvardi, M. K.; Stitt, M. Genome-wide reprogramming of primary and secondary metabolism, protein synthesis, cellular growth processes, and the regulatory infrastructure of *Arabidopsis* in response to nitrogen. *Plant Physiol.* **2004**, *136* (1), 2483–2499.
- (13) Stewart, V. Regulation of nitrate and nitrite reductase synthesis in enterobacteria. *Antonie van Leeuwenhoek* **1994**, *66* (1), 37–45.
- (14) Feng, B.; Marzluf, G. A. Interaction between major nitrogen regulatory protein NIT2 and pathway-specific regulatory factor NIT4 is required for their synergistic activation of gene expression in *Neurospora crassa*. *Mol. Cell. Biol.* **1998**, *18* (7), 3983–3990.
- (15) Camargo, A.; Llamas, A.; Schnell, R. A.; Higuera, J. J.; Gonzalez-Ballester, D.; Lefebvre, P. A.; Fernandez, E.; Galvan, A. Nitrate signalling by the regulatory gene NIT2 in *Chlamydomonas*. *Plant Cell* **2007**, *19* (11), 3491–3503.
- (16) Ho, C.-H.; Lin, S.-H.; Hu, H.-C.; Tsay, Y.-F. CHL1 functions as a nitrate sensor in plants. *Cell* **2009**, *138* (6), 1184–1194.
- (17) Wang, R.; Xing, X.; Wang, Y.; Tran, A.; Crawford, N. M. A genetic screen for nitrate regulatory mutants captures the nitrate transporter gene NRT1.1. *Plant Physiol.* **2009**, *151* (1), 472–478.
- (18) Little, D. Y.; Rao, H.; Oliva, S.; Daniel-Vedele, F.; Krapp, A.; Malamy, J. E. The putative high-affinity nitrate transporter NRT2.1 represses lateral root initiation in response to nutritional cues. *Proc. Natl. Acad. Sci. U.S.A.* **2005**, *102* (38), 13693–13698.
- (19) Widiez, T.; El Kafafi, E. S.; Girin, T.; Berr, A.; Ruffel, S.; Krouk, G.; Vayssières, A.; Shen, W.-H.; Coruzzi, G. M.; Gojon, A.; Lepetit, M. HIGH NITROGEN INSENSITIVE 9 (HNI9)-mediated systemic repression of root  $\text{NO}_3^-$  uptake is associated with changes in histone methylation. *Proc. Natl. Acad. Sci. U.S.A.* **2011**, *108* (32), 13329–13334.
- (20) Castaings, L.; Camargo, A.; Pocholle, D.; Gaudon, V.; Texier, Y.; Boutet-Mercey, S.; Taconnat, L.; Renou, J. P.; Daniel-Vedele, F.; Fernandez, E.; Meyer, C.; Krapp, A. The nodule inception-like protein 7 modulates nitrate sensing and metabolism in *Arabidopsis*. *Plant J.* **2009**, *57* (3), 426–435.
- (21) Hu, H. C.; Wang, Y. Y.; Tsay, Y. F. AtCIPK8, a CBL-interacting protein kinase, regulates the low-affinity phase of the primary nitrate response. *Plant J.* **2009**, *57* (2), 264–278.
- (22) Zhang, H.; Forde, B. G. An *Arabidopsis* MADS box gene that controls nutrient-induced changes in root architecture. *Science* **1998**, *279* (5349), 407–409.
- (23) Gutierrez, R. A.; Stokes, T. L.; Thum, K.; Xu, X.; Obertello, M.; Katari, M. S.; Tanurdzic, M.; Dean, A.; Nero, D. C.; McClung, C. R.; Coruzzi, G. M. Systems approach identifies an organic nitrogen-responsive gene network that is regulated by the master clock control gene CCA1. *Proc. Natl. Acad. Sci. U.S.A.* **2008**, *105* (12), 4939–4944.
- (24) Gifford, M. L.; Dean, A.; Gutierrez, R. A.; Coruzzi, G. M.; Birnbaum, K. D. Cell-specific nitrogen responses mediate developmental plasticity. *Proc. Natl. Acad. Sci. U.S.A.* **2008**, *105* (2), 803–808.
- (25) Pant, B. D.; Musialak-Lange, M.; Nuc, P.; May, P.; Buhtz, A.; Kehr, J.; Walther, D.; Scheible, W. R. Identification of nutrient-responsive *Arabidopsis* and rapeseed microRNAs by comprehensive real-time polymerase chain reaction profiling and small RNA sequencing. *Plant Physiol.* **2009**, *150* (3), 1541–1555.

- (26) Peng, M.; Hannam, C.; Gu, H.; Bi, Y. M.; Rothstein, S. J. A mutation in *NLA*, which encodes a RING-type ubiquitin ligase, disrupts the adaptability of *Arabidopsis* to nitrogen limitation. *Plant J.* **2007**, *50* (2), 320–337.
- (27) Peng, M.; Hudson, D.; Schofield, A.; Tsao, R.; Yang, R.; Gu, H.; Bi, Y.-M.; Rothstein, S. J. Adaptation of *Arabidopsis* to nitrogen limitation involves induction of anthocyanin synthesis which is controlled by the *NLA* gene. *J. Exp. Bot.* **2008**, *59* (11), 2933–2944.
- (28) Wegener, K. M.; Singh, A. K.; Jacobs, J. M.; Elvitigala, T.; Welsh, E. A.; Keren, N.; Gritsenko, M. A.; Ghosh, B. K.; Camp, D. G. II; Smith, R. D.; Pakrasi, H. B. Global proteomics reveal an atypical strategy for carbon/nitrogen assimilation by a cyanobacterium under diverse environmental perturbations. *Mol. Cell. Proteomics* **2010**, *9* (12), 2678–2689.
- (29) Rampitsch, C.; Subramaniam, R.; Djuric-Ciganovic, S.; Bykova, N. V. The phosphoproteome of *Fusarium graminearum* at the onset of nitrogen starvation. *Proteomics* **2009**, *10* (1), 124–140.
- (30) Lin, W. Y.; Chang, J. Y.; Hish, C. H.; Pan, T. M. Profiling the *Monascus pilosus* proteome during nitrogen limitation. *J. Agric. Food Chem.* **2008**, *56* (2), 433–441.
- (31) Prinsi, B.; Negri, A. S.; Pesaresi, P.; Cocucci, M.; Espen, L. Evaluation of protein pattern changes in roots and leaves of *Zea mays* plants in response to nitrate availability by two-dimensional gel electrophoresis analysis. *BMC Plant Biol.* **2009**, *9*, 113.
- (32) MØller, A. L. B.; Pedas, P. A. I.; Andersen, B.; Svensson, B.; Schjoerring, J. K.; Finnie, C. Responses of barley root and shoot proteomes to long-term nitrogen deficiency, short-term nitrogen starvation and ammonium. *Plant Cell Environ.* **2011**, *34* (12), 2024–2037.
- (33) Bahrman, N.; Gouy, A.; Devienne-Barret, F.; Hirel, B.; Vedele, F.; Gouis, J. L. Differential change in root protein patterns of two wheat varieties under high and low nitrogen nutrition levels. *Plant Sci.* **2005**, *168* (1), 81–87.
- (34) Kusano, M.; Fukushima, A.; Redestig, H.; Saito, K. Metabolomic approaches toward understanding nitrogen metabolism in plants. *J. Exp. Bot.* **2011**, *62* (4), 1439–1453.
- (35) Gallois, J. L.; Guyon-Debast, A.; Lecureuil, A.; Vezon, D.; Carpentier, V.; Bonhomme, S.; Guerche, P. The *Arabidopsis* proteasome RPT5 subunits are essential for gametophyte development and show accession-dependent redundancy. *Plant Cell* **2009**, *21* (2), 442–459.
- (36) Schlesier, B.; Berna, A.; Bernier, F.; Mock, H. P. Proteome analysis differentiates between two highly homologues germin-like proteins in *Arabidopsis thaliana* ecotypes Col-0 and Ws-2. *Phytochemistry* **2004**, *65* (11), 1565–1574.
- (37) Zor, T.; Selinger, Z. Linearization of the Bradford protein assay increases its sensitivity: theoretical and experimental studies. *Anal. Biochem.* **1996**, *236* (2), 302–308.
- (38) Fitter, D. W.; Martin, D. J.; Copley, M. J.; Scotland, R. W.; Langdale, J. A. *GLK* gene pairs regulate chloroplast development in diverse plant species. *Plant J.* **2002**, *31* (6), 713–727.
- (39) Sunkar, R.; Kapoor, A.; Zhu, J. K. Posttranscriptional induction of two Cu/Zn superoxide dismutase genes in *Arabidopsis* is mediated by downregulation of miR398 and important for oxidative stress tolerance. *Plant Cell* **2006**, *18* (8), 2051–2065.
- (40) Deng, Z.; Zhang, X.; Tang, W.; Oses-Prieto, J. A.; Suzuki, N.; Gendron, J. M.; Chen, H.; Guan, S.; Chalkley, R. J.; Peterman, T. K.; Burlingame, A. L.; Wang, Z. Y. A proteomics study of brassinosteroid response in *Arabidopsis*. *Mol. Cell. Proteomics* **2007**, *6* (12), 2058–2071.
- (41) Ma, Y.; Yu, J.; Chan, H. L.; Chen, Y. C.; Wang, H.; Chen, Y.; Chan, C. Y.; Go, M. Y.; Tsai, S. N.; Ngai, S. M.; To, K. F.; Tong, J. H.; He, Q. Y.; Sung, J. J.; Kung, H. F.; Cheng, C. H.; He, M. L. Glucose-regulated protein 78 is an intracellular antiviral factor against hepatitis B virus. *Mol. Cell. Proteomics* **2009**, *8* (11), 2582–2594.
- (42) Agrawal, G. K.; Thelen, J. J. Development of a simplified, economical polyacrylamide gel staining protocol for phosphoproteins. *Proteomics* **2005**, *5* (18), 4684–4688.
- (43) Candiano, G.; Bruschi, M.; Musante, L.; Santucci, L.; Ghiggeri, G. M.; Carnemolla, B.; Orecchia, P.; Zardi, L.; Righetti, P. G. Blue silver: a very sensitive colloidal Coomassie G-250 staining for proteome analysis. *Electrophoresis* **2004**, *25* (9), 1327–1333.
- (44) Yu, Z. Y.; Han, G. H.; Sun, S. T.; Jiang, X. N.; Chen, R.; Wang, F. J.; Wu, R. A.; Ye, M. L.; Zou, H. F. Preparation of monodisperse immobilized Ti<sup>4+</sup> affinity chromatography microspheres for specific enrichment of phosphopeptides. *Anal. Chim. Acta* **2009**, *636* (1), 34–41.
- (45) Han, G. H.; Ye, M. L.; Zhou, H. J.; Jiang, X. N.; Feng, S.; Jiang, X. G.; Tian, R. J.; Wan, D. F.; Zou, H. F.; Gu, J. R. Large-scale phosphoproteome analysis of human liver tissue by enrichment and fractionation of phosphopeptides with strong anion exchange chromatography. *Proteomics* **2008**, *8* (7), 1346–1361.
- (46) Jiang, X.; Ye, M.; Cheng, K.; Zou, H. ArMone: a software suite specially designed for processing and analysis of phosphoproteome data. *J. Proteome Res.* **2010**, *9* (5), 2743–2751.
- (47) Jiang, X.; Han, G.; Feng, S.; Ye, M.; Yao, X.; Zou, H. Automatic validation of phosphopeptide identifications by the MS2/MS3 target-decoy search strategy. *J. Proteome Res.* **2008**, *7* (4), 1640–1649.
- (48) Saeed, A. I.; Bhagabati, N. K.; Braisted, J. C.; Liang, W.; Sharov, V.; Howe, E. A.; Li, J.; Thiagarajan, M.; White, J. A.; Quackenbush, J. TM4 microarray software suite. *Methods Enzymol.* **2006**, *411*, 134–93.
- (49) Szklarczyk, D.; Franceschini, A.; Kuhn, M.; Simonovic, M.; Roth, A.; Minguez, P.; Doerks, T.; Stark, M.; Muller, J.; Bork, P.; Jensen, L. J.; Mering, C. v. The STRING database in 2011: functional interaction networks of proteins, globally integrated and scored. *Nucleic Acids Res.* **2011**, *39* (Suppl. 1), D561–D568.
- (50) Heazlewood, J. L.; Verboom, R. E.; Tonti-Filippini, J.; Small, I.; Millar, A. H. SUBA: the *Arabidopsis* Subcellular Database. *Nucleic Acids Res.* **2007**, *35* (Database issue), D213–218.
- (51) Heazlewood, J. L.; Durek, P.; Hummel, J.; Selbig, J.; Weckwerth, W.; Walther, D.; Schulze, W. X. PhosPhAt: a database of phosphorylation sites in *Arabidopsis thaliana* and a plant-specific phosphorylation site predictor. *Nucleic Acids Res.* **2008**, *36* (Suppl. 1), D1015–D1021.
- (52) Potel, F.; Valadier, M. H.; Ferrario-Mery, S.; Grandjean, O.; Morin, H.; Gaufichon, L.; Boutet-Mercey, S.; Lothier, J.; Rothstein, S. J.; Hirose, N.; Suzuki, A. Assimilation of excess ammonium into amino acids and nitrogen translocation in *Arabidopsis thaliana*—roles of glutamate synthases and carbamoylphosphate synthetase in leaves. *FEBS J.* **2009**, *276* (15), 4061–4076.
- (53) Ribeiro, D. T.; Farias, L. P.; de Almeida, J. D.; Kashiwabara, P. M.; Ribeiro, A. F. C.; Silva-Filho, M. C.; Menck, C. F. M.; Van Sluys, M.-A. Functional characterization of the *thi1* promoter region from *Arabidopsis thaliana*. *J. Exp. Bot.* **2005**, *56* (417), 1797–1804.
- (54) Buchanan, B. B.; Balmer, Y. Redox regulation: a broadening horizon. *Annu. Rev. Plant Biol.* **2005**, *56*, 187–220.
- (55) Vanderauwera, S.; Zimmermann, P.; Rombauts, S.; Vandenabeele, S.; Langebartels, C.; Grussem, W.; Inze, D.; Van Breusegem, F. Genome-wide analysis of hydrogen peroxide-regulated gene expression in *Arabidopsis* reveals a high light-induced transcriptional cluster involved in anthocyanin biosynthesis. *Plant Physiol.* **2005**, *139* (2), 806–821.
- (56) Beauclair, L.; Yu, A.; Bouche, N. microRNA-directed cleavage and translational repression of the copper chaperone for superoxide dismutase mRNA in *Arabidopsis*. *Plant J.* **2010**, *62* (3), 454–62.
- (57) Dugardeyn, J.; Vandenbussche, F.; Van Der Straeten, D. To grow or not to grow: what can we learn on ethylene-gibberellin cross-talk by *in silico* gene expression analysis? *J. Exp. Bot.* **2008**, *59* (1), 1–16.
- (58) Ruzicka, K.; Ljung, K.; Vanneste, S.; Podhorska, R.; Beeckman, T.; Friml, J.; Benkova, E. Ethylene regulates root growth through effects on auxin biosynthesis and transport-dependent auxin distribution. *Plant Cell* **2007**, *19* (7), 2197–2212.
- (59) Wang, P.; Du, Y.; Li, Y.; Ren, D.; Song, C. P. Hydrogen peroxide-mediated activation of MAP kinase 6 modulates nitric oxide biosynthesis and signal transduction in *Arabidopsis*. *Plant Cell* **2010**, *22* (9), 2981–2998.

- (60) Xing, Y.; Jia, W.; Zhang, J. AtMKK1 mediates ABA-induced *CAT1* expression and H<sub>2</sub>O<sub>2</sub> production via AtMPK6-coupled signaling in *Arabidopsis*. *Plant J.* **2008**, *54* (3), 440–451.
- (61) Kolbert, Z.; Bartha, B.; Erdei, L. Exogenous auxin-induced NO synthesis is nitrate reductase-associated in *Arabidopsis thaliana* root primordia. *J. Plant Physiol.* **2008**, *165* (9), 967–975.
- (62) Signora, L.; De Smet, I.; Foyer, C. H.; Zhang, H. ABA plays a central role in mediating the regulatory effects of nitrate on root branching in *Arabidopsis*. *Plant J.* **2001**, *28* (6), 655–662.
- (63) Mortimer, J. C.; Laohavosit, A.; Macpherson, N.; Webb, A.; Brownlee, C.; Battey, N. H.; Davies, J. M. Annexins: multifunctional components of growth and adaptation. *J. Exp. Bot.* **2008**, *59* (3), 533–544.
- (64) Lin, Y.; Cheng, C. L. A chlorate-resistant mutant defective in the regulation of nitrate reductase gene expression in *Arabidopsis* defines a new HY locus. *Plant Cell* **1997**, *9* (1), 21–35.
- (65) Cao, D.; Lin, Y.; Cheng, C. L. Genetic interactions between the chlorate-resistant mutant *cr* 8 and the photomorphogenic mutants *cop1* and *hy5*. *Plant Cell* **2000**, *12* (2), 199–210.
- (66) Cai, W.; Ma, J.; Guo, J.; Zhang, L. Function of ROC4 in the efficient repair of photodamaged photosystem II in *Arabidopsis*. *Photochem. Photobiol.* **2008**, *84* (6), 1343–1348.
- (67) Engelsberger, W. R.; Schulze, W. X. Nitrate and ammonium lead to distinct global dynamic phosphorylation patterns when resupplied to nitrogen starved *Arabidopsis* seedlings. *Plant J.* **2012**, DOI: 10.1111/j.1365-313X.2011.04848.x.
- (68) Wollman, F. A. State transitions reveal the dynamics and flexibility of the photosynthetic apparatus. *EMBO J.* **2001**, *20* (14), 3623–3630.